Release of Corrosive Species above the Grate in a Waste Boiler and the Implication for Improved Electrical Efficiency

Bøjer, Martin; Jensen, Peter Arendt; Dam-Johansen, Kim; Madsen, Ole Hedegaard; Lundtorp, Kasper

Published in:
Energy & Fuels

Link to article, DOI:
10.1021/ef1003655

Publication date:
2010

Document Version
Publisher's PDF, also known as Version of record

Energy Fuels **2010,** *24,* 5696–5707 · DOI:10.1021/ef1003655
Published on Web 09/28/2010

energy&fuels
article

Release of Corrosive Species above the Grate in a Waste Boiler and the Implication for Improved Electrical Efficiency

Martin Bøjer,[†] Peter Arendt Jensen,*[,†] Kim Dam-Johansen,[†] Ole Hedegaard Madsen,[‡] and Kasper Lundtorp[‡]

[†]*Combustion and Harmful Emission Control (CHEC) Research Centre, Department of Chemical and Biochemical Engineering, Technical University of Denmark, Building 229, DK-2800 Kgs. Lyngby, Denmark, and* [‡]*Babcock and Wilcox Vølund A/S, Odinsvej 19, DK-2600 Glostrup, Denmark*

Received March 29, 2010. Revised Manuscript Received August 30, 2010

A relatively low electrical efficiency of 20−25% is obtained in typical west European waste boilers. Ash species released from the grate combustion zone form boiler deposits with high concentrations of Cl, Na, K, Zn, Pb, and S that cause corrosion of superheater tubes at high temperature. The superheater steam temperature has to be limited to around 425 °C, and thereby, the electrical efficiency remains low compared to wood or coal-fired boilers. If a separate part of the flue gas from the grate has a low content of corrosive species, it may be used to superheat steam to a higher temperature, and thereby, the electrical efficiency of the plant can be increased. In this study, the local temperature, the gas concentrations of CO, CO_2, and O_2, and the release of the volatile elements Cl, S, Na, K, Pb, Zn, Cu, and Sn were measured above the grate in a waste boiler to investigate if a selected fraction of the flue gas could be applied for increased steam superheating. On a 26 ton/h grate-fired waste boiler, Vestforbrænding unit 5 in Denmark, local probe measurements were performed in five ports along the grate and in the top of the boiler chamber. New extraction probe equipment were designed and used to extract a flue gas with high contents of tar. Gas concentration measurements of O_2, CO, and CO_2 showed that the waste experienced pyrolysis and combustion on grate sections 1 and 2, some char combustion takes place on section 3, and the slag was cooled on sections 4 and 5. The measurements showed that the waste grate combustion process can provide a flue gas with a high energy content and a relatively low concentration of corrosive species. This opens up for the possibility of using an additional superheater section to increase the steam temperature and, thereby, increase electrical efficiency.

Introduction

Combined heat and electricity producing waste-to-energy (WtE) boilers cause less fossil-fuel-based CO_2 emissions per produced megawatt hour (MWh) than plants based on fossil fuels. The WtE boilers also reduce the emission of methane from waste landfill sites, which is a 21 times more efficient greenhouse gas (GHG) compared to CO_2 (over a 100 year period).[1]

Because of corrosive deposits forming on the superheater surfaces,[2] the superheater steam temperature in WtE boilers is usually kept below approximately 420 °C to minimize corrosion, which would otherwise require frequent replacement of superheaters.[3] At a superheated steam temperature of approximately 380−420 °C and 50 bar, an electrical efficiency of 20−25% is obtained.[4]

The background for this work was founded on a patent owned by Babcock and Wilcox Vølund.[5] Figure 1 shows the principle of the patent. Corrosive constituents are released early in the combustion process. The remaining combustion on the grate will thus create a relatively clean flue gas free of the majority of corrosive constituents while still maintaining a relatively high temperature. In the new proposed design, a barrier is inserted to form two fractions of the flue gas, one fraction containing higher than average contents of corrosive constituents and one fraction containing a lower than average amount of corrosive constituents. This clean flue gas could then be directed to an extra superheater section inserted in the first draft of the boiler. This additional superheater section would receive steam from the conventional superheater sections and enable an increased final steam temperature.

Information on the release of the volatile corrosive species and the temperature profile along the grate are important to evaluate the placement of the barrier, as shown in Figure 1.

On the pilot-plant TAMARA, flue gas samples were taken along the grate but no data have been released on the concentration of corrosive elements.[6]

In 2005, a few concentration measurements of Cl, Na, K, Ca, S, Pb, and Zn were carried out above the grate at the Vestforbrænding unit 5.[4,7,8] Some limitations of the measurement equipment were experienced during those experiments.

*To whom correspondence should be addressed. Telephone: +45-4525-2849. Fax: +45-4588-2258. E-mail: paj@kt.dtu.dk.

(1) United States Environmental Protection Agency (U.S. EPA). http://epa.gov/methane/ (accessed in 2008).
(2) Spiegel, M. *Mater. Corros.* **1999**, *50*, 373–393.
(3) Born, M. *VGB PowerTech* **2005**, *5*, 107–111.
(4) Madsen, O. H.; Bøjer, M.; Jensen, P. A.; Dam-Johansen, K. High electrical efficiency by dividing the combustion products. *Proceedings of the 16th Annual North American Waste-to-Energy Conference* (*NAWTEC*); Philadelphia, PA, May 19−21, 2008.
(5) Dam-Johansen, K. A.; Jensen, P. A.; Frandsen, F. J.; Madsen, O. H. A boiler producing steam from flue gases with high electrical efficiency and improved slag quality. Application number EP20060809447, 2006.
(6) Frey, H.-H.; Peters, B.; Hunsinger, H.; Vehlow, J. *Waste Manage.* **2003**, *23*, 689–701.
(7) Bøjer, M.; Jensen, P. A.; Frandsen, F.; Dam-Johansen, K.; Madsen, O. H.; Lundtorp, K. Release of potentially corrosive constituents from the grate of a waste-to-energy boiler. *IT3 2007 Conference*; Phoenix, AZ, May 14−18, 2007.

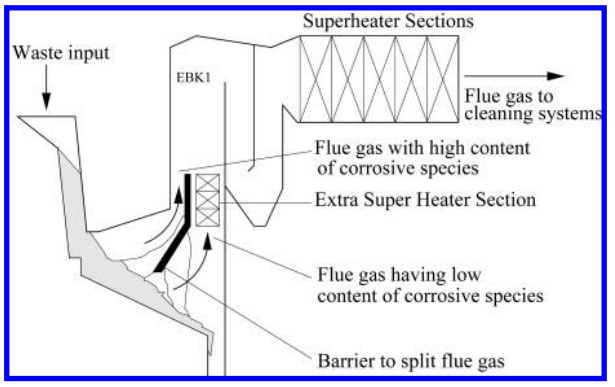

Figure 1. Schematic of the Babcock and Wilcox Vølund owned patent for elevating the superheated steam temperature/pressure using the non-corrosive fraction of the flue gas.

It was not possible to reuse the probes during the experiments, and therefore, only a limited number of experiments was conducted with no reproduction of the obtained results. The probes were not reused because of condensation of tar-like material inside the colder parts (<100 °C) of the sampling system. The condensed tar/char resulted in additional work required to extract the tar from the sampling probes and additional uncertainty of the chemical analysis. The new experiments remedied this deficiency by providing multiple measurements at each location using a newly designed probe that significantly reduced the tar condensation problems.

The objectives of this work are to provide information on the concentration of corrosive species along the grate and the energy release rate along the grate. Also, it is of interest to determine the overall concentration of corrosive constituents in the fully mixed flue gas in the top of the furnace chamber. It will be evaluated whether it is possible to find a suitable location for the barrier with regard to the design shown in Figure 1 and whether there will be sufficient heat available for the additionally inserted superheater section.

Because of a high tar content directly above the bed that causes fouling in conventional flue gas extraction probes, a new tar-tolerant probe was developed. Analysis of the recorded video of the grate combustion during operation was used to document the position of the flames. To investigate the impact of extended grate fire, it was desired to use two different operating conditions: a normal grate fire operation and an extended grate fire operation.

Experimental Section

All measurements were conducted at Vestforbrænding unit 5, a heat and power generating WtE plant in Glostrup, Denmark. Table 1 shows specifications for the plant that was commissioned in 1998. The refuse was incinerated on a hydraulically operated forward-acting grate, which is 9.75 m wide and 13.1 m long and consists of 18 zones. Each zone was supplied with individually controlled primary air (see dimensions in Figure 2). The control room manually regulated the volumetric flow rate for either specific zones or groups of zones. Ammonia was injected in the first draft to reduce NO_x.

The refuse originated from Copenhagen households and companies. The refuse was mixed by three automatic operated cranes. No further sorting or treatment of the refuse was performed. The measurements were performed during, for Danish conditions, a particularly rainy July in 2007, achieving approximately 160 mm of rain for the entire month in the area of the plant.[9]

The measurement positions seen in Figure 2 were situated 154, 161, 172, 182, 169, and 154 cm above the grate for ports L1−L6. The tip of the probe was inserted at a depth of 160 cm from the boiler wall, and the ports L1−L6 were placed in the middle of the grate zones. Multiple measurement positions were located in the top of the first draft (EBK1), of which the center position was used.

Plant Operation. During the experiments, the unit 5 boiler was running stable and did not experience malfunctions. Data collected from the plant control system showed that the electrical energy production was 12.6 ± 2.1 MW. The steam pressure was 50.0 ± 0.5 bar, and the steam production was 96.0 ± 8.3 t h^{-1}, which are normal levels for the boiler unit. The impact of the wet refuse because of the rainy season could be observed from the average lower heating value (LHV) of 10.84 MJ kg^{-1} of the plant compared to an average of 11.62 MJ kg^{-1} observed in the 2005 experiments, which was a drier season.[8]

Primary, secondary, and recirculation air flow measurements were obtained from the plant surveillance and control system. The flow of secondary air and recirculation flue gas intruding directly above the grate were closed.

Table 1. Vestforbrænding Unit 5 Specifications

nominal capacity (tons h^{-1})	26
nominal energy production[a] (MW)	66
nominal electricity production (MW)	16
steam pressure (bar)	55
steam temperature (°C)	380
primary air flow (N m^3 h^{-1})	up to 154700
average share of primary air to sections L1−L6 (%)	3.2, 7.8, 9.0, 7.6, 6.1, and 1.7
primary air temperature (°C)	approximately 120
secondary air flow (N m^3 h^{-1})	up to 46400
recirculated flue gas[b] (N m^3 h^{-1})	up to ∼112000
recirculated flue gas temperature (°C)	180
grate type	Vølund grate

[a] At a lower heating value (LHV) of 12 MJ kg^{-1}. [b] Up to 27% of clean flue gases after the electrostatic precipitator.

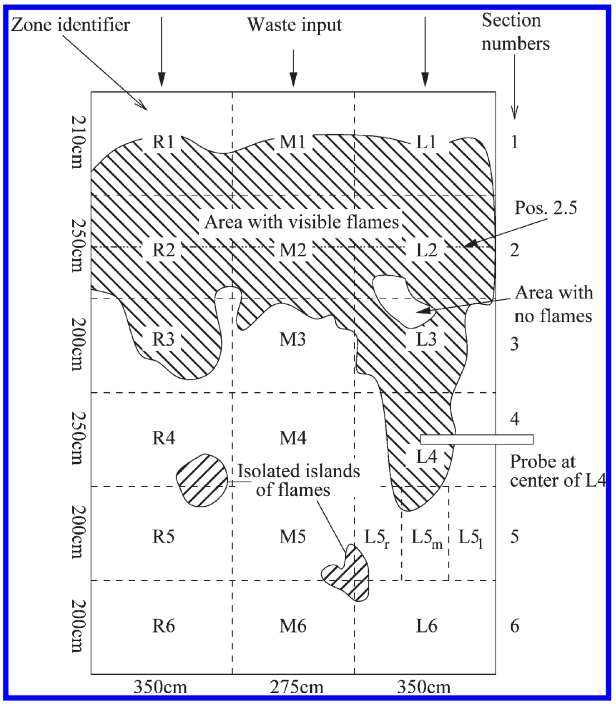

Figure 2. Sketch of the flame zones across the grate.

(8) Bøjer, M.; Jensen, P. A.; Frandsen, F.; Dam-Johansen, K.; Madsen, O. H.; Lundtorp, K. *Fuel Process. Technol.* **2008**, *89*, 528–539.
(9) Danmarks Meteorologiske Institut (DMI). http://www.dmi.dk/ (accessed in 2007).

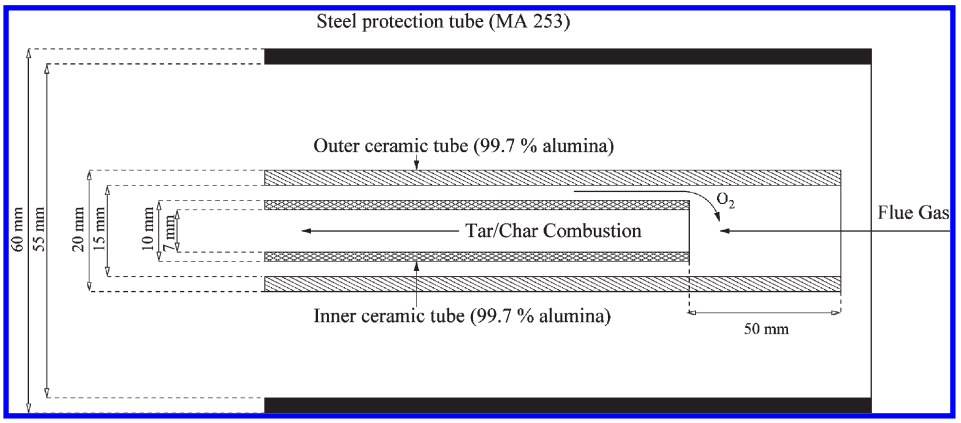

Figure 3. Probe type S1 with the ability to inject oxygen at the tip of the probe.

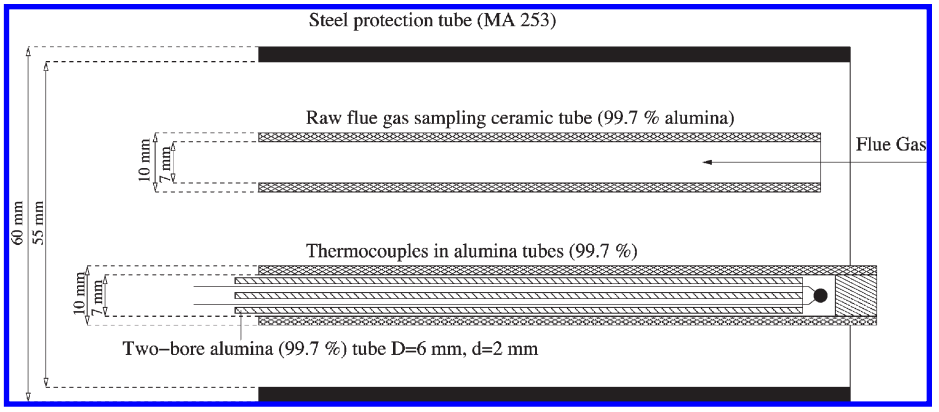

Figure 4. Probe type S2 with the ability to sample raw flue gas and to measure temperature simultaneously.

A video recording was made of the grate using the internal video surveillance system of the plant. The view of the flame positions on the grate was used in the control room as a reference for controlling the combustion process. In this study, the video recordings were used to determine the actual position of the flame front during the probe measurements. Every 10th minute, a frame of the video of the grate combustion was manually analyzed by dividing each of the zones into smaller sub-zones and the position of the edge of the visual flames was noted. As an example, a value of 2.5 is interpreted as the middle of the second zone.

Large variations of the position of the visual flames were observed during the probe measurements. Combustion was highly irregular across the grate. Figure 2 shows how tongues of flames would sometimes stretch along parts of the grate, while also small islands of flames could exist further down the grate beyond the flame front.

Flue Gas Sampling Systems. Because of space limitations of the measurement ports, two different probe types S1 and S2 were used to sample flue gas and measure the concentration of volatile Cl, Na, K, S, Pb, Zn, Ca, Sn, and Cu, local flue gas temperature, and the concentrations of CO, CO_2, O_2, NO, and SO_2 in the flue gas. The probes used do not have filters mounted at the tip because the filter within a short time (10−15 min) would close up as a result of the amount of particles in the flue gas this close to the fuel bed.

Probe type S1 was designed to combust tar/char from the flue gas by injecting oxygen at the tip of the probe inside the boiler when tar was present in the flue gas at temperatures above 800 °C, allowing the tar to be combusted. Figure 3 shows the tip of the probe type S1 in which oxygen was added.

Probe type S2 was designed to sample flue gas for measuring the gas concentrations of CO, CO_2, O_2, NO, and SO_2 and make simultaneous temperature measurements. Figure 4 shows the design of probe type S2. The temperature was measured using a Pt/Rh thermocouple.

A partly water-cooled probe container was designed to accommodate probes S1 and S2. Figure 5 shows the water-cooled probe container mounted with the probe type S1. The water cooling was necessary because earlier experiments in the project with other probe designs showed that a full-length outer tube made of MA 253 steel without water cooling would otherwise bend inside the boiler. Two of these water-cooled probe containers were made, and it was therefore possible to run two concurrent experiments at two different ports. It was chosen to run the experiments at adjacent ports using either a probe type S1 or S2 in both of the ports because they could then be directly compared.

Figure 6 shows the general layout of the sampling system when using probe type S1. The oxygen injection (1) can be added to the probe via the mass flow controller (MFC) (2).

The flue gas/oxygen enters the inner probe tube and passes through an electrically heated glass container filled with laboratory-grade quartz wool (5). The flue gas enters an optional 3−4 wash bottles with absorber solution (6), which absorbs constituents from the flue gas. Downstream from the absorber bottles, the flue gas enters a gas treatment system (7−13). The gas treatment system consists of a heated filter (7), a water condenser (8), a "cold" filter (9), a membrane pump (10), a mass flow controller (11), and a ball flow meter (13). After the gas treatment system, a CO, CO_2, and O_2 Rosemount NGA 2000 gas analyzer (14) is attached. An optional NO and SO_2 Rosemount NGA 2000 (15) can be attached. Finally, a gas volume meter/counter (16) was used to measure the total flue gas volume over a given period of time.

The S2 sampling system has the ability to sample flue gas and measure the temperature simultaneously. Figure 4 shows this concept, where two separate tubes are inserted. The flue

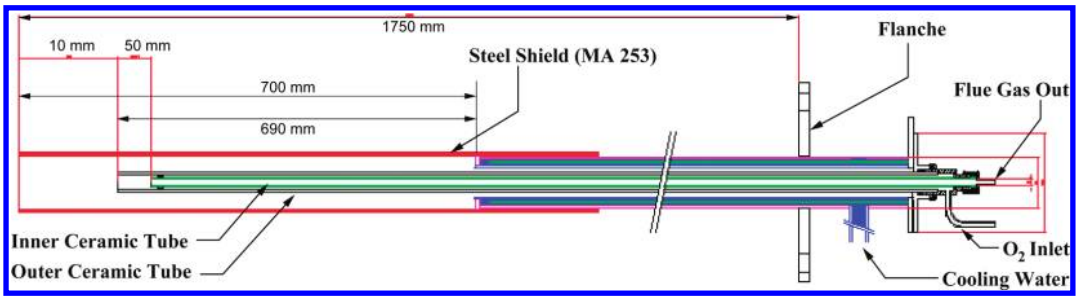

Figure 5. Generic water-cooled probe, mounted here with probe type S1 for sampling tar/char-rich flue gas by injecting oxygen at the tip of the probe.

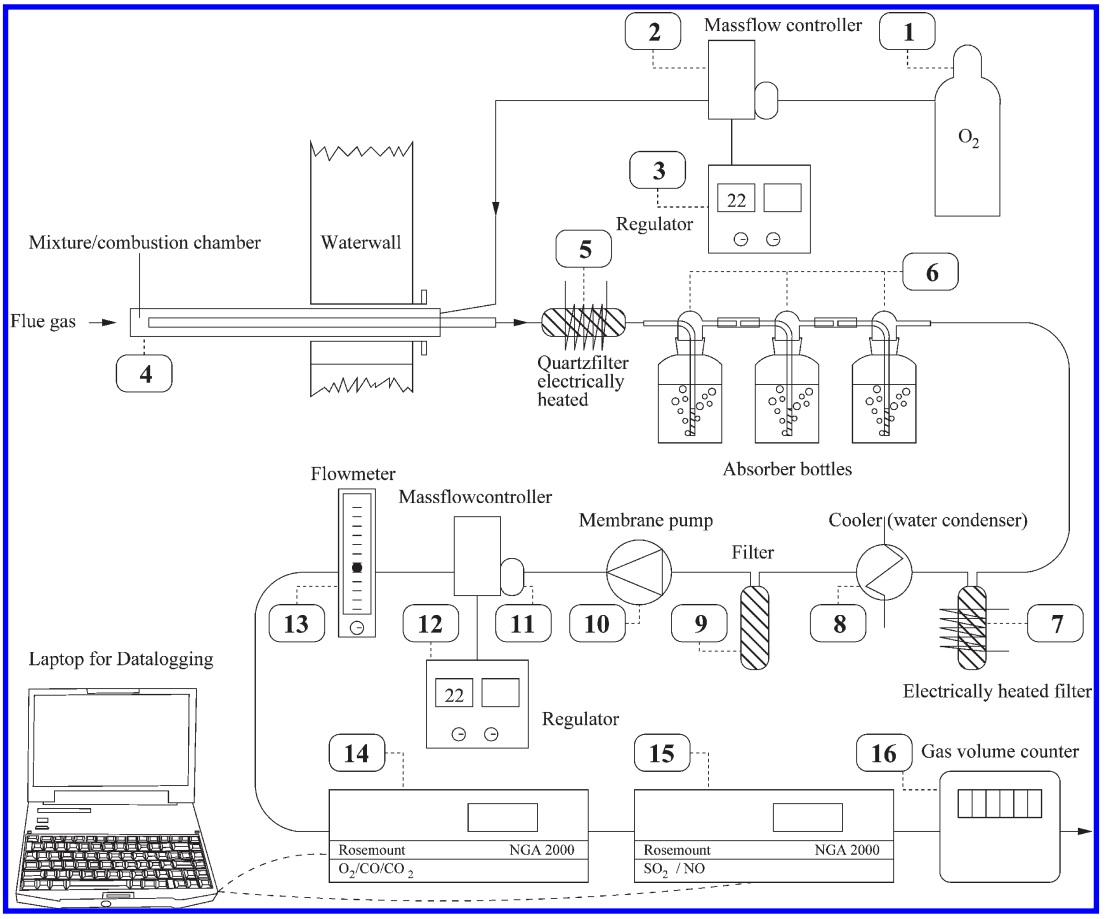

Figure 6. Overall design of the S1 sampling system using a probe with optional oxygen injection.

gas was passed through two wash bottles containing only pure water (double-distilled 18 mΩ) to minimize particles entering the sampling system. Figure 7 shows the S2 sampling system.

The differences between systems 1 and 2 are the probe type (1 and 4), the thermocouples (1 and 2), the temperature unit (3), no oxygen injection, and the wash bottles (6) containing purified water only.

In some cases (sampling IDs 28 and 29) when the sampling system 2 is used together with the absorber bottles containing absorption liquids (6), an asterisk (∗) is added to the S2, thus becoming sampling system S2*. This system is only used when no tar is present in the flue gas.

Sampling of Cl, S, Na, K, Ca, Zn, Pb, Cu, and Sn was performed using the two absorption liquids described in Table 2.

The probe design (see Figure 5) was created mainly for extraction of gas-phase species. However, some aerosols may also be extracted.

To make repeated experiments, two or more measurements with gas absorption, $CO/CO_2/O_2$ concentrations, and temperature were performed at ports L2−L4.

Results and Discussion

In this section, validation of measurements with the probe S1 with oxygen injection will be discussed. Then, the flame position determination, gas concentration profiles, and release profiles of the volatile constituents Cl, S, Na, K, Pb, Zn, Sn, and Cu will be shown and discussed. A determination of the concentration of corrosive constituents in the fully developed flue gas is compared to the measured grate concentrations.

Validation of Oxygen Injection. To test the tar/char removal of the flue gas in probe S1, oxygen was injected and outlet CO, CO_2, and O_2 concentrations were measured in

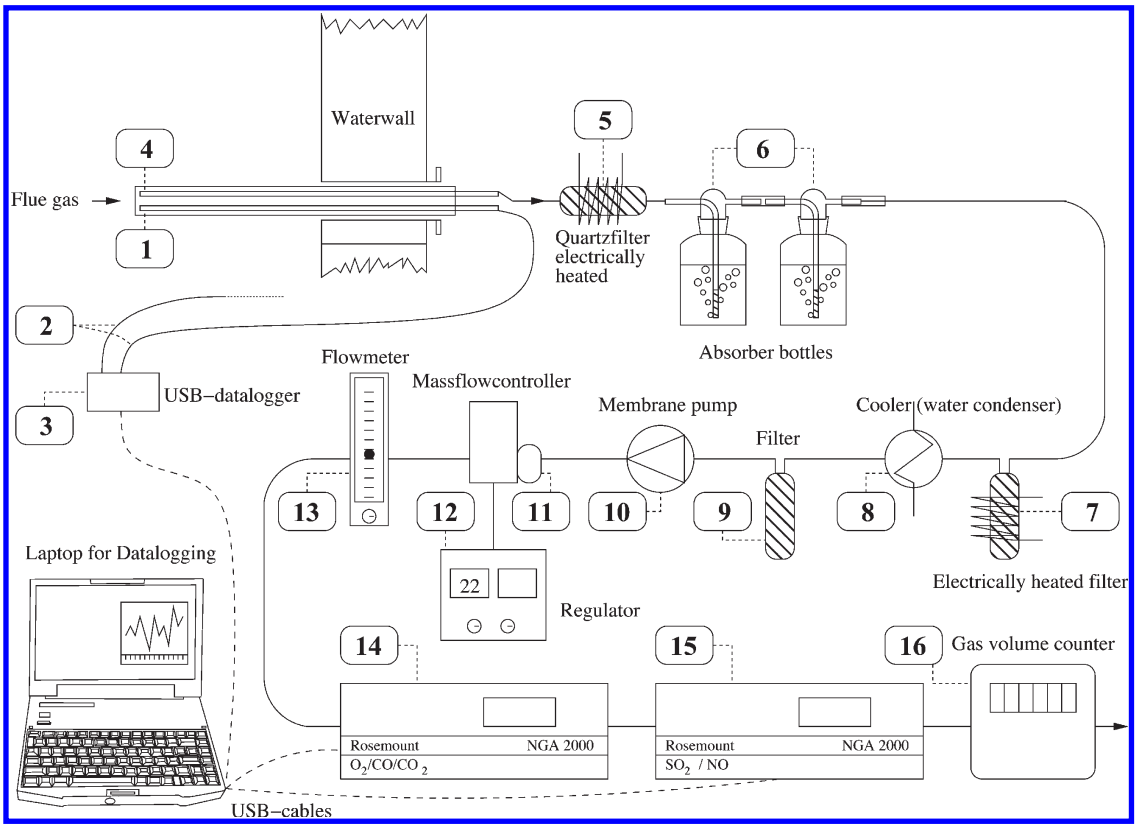

Figure 7. Overall design of the S2 sampling system.

Table 2. Target Absorption Elements, Wash Bottle Solutions, and Corresponding Solution Standard

Cl, Na, K, and Ca	0.75% NH_3	DS/EN 1911 using NH_3 instead of NaOH
Pb, Zn, Cu, Sn, and S	4.5% HNO_3 and 1.7% H_2O_2	EN 14385 and ISO 11632

port L2, which contained a significant amount of tar/char in the flue gas. For the oxygen injection to be successful, the CO level must be reduced to relatively low levels and tar/char in the sampling systems must be minimized, so that it does not foul the sampling system.

The performance of probe type S1 with oxygen injection is shown by comparing CO, CO_2, and O_2 concentrations to those of probe type S2 without oxygen injection at port L2. Figure 8 shows graphs of the concentration of CO, CO_2, and O_2 and the temperature using probe type S2, which did not use oxygen injection. The CO concentration was 6.9 ± 0.8 vol %, and the O_2 concentration was 0.14 ± 0.09 vol %. Figure 9 shows graphs of the concentration of CO, CO_2, and O_2 during a measurement using probe type S1 with oxygen injection. The CO concentration was 67 ± 150 ppm_v, and the O_2 concentration was 26.7 ± 5.9 vol %. The oxygen levels occasionally reached the maximum concentration limit of the gas analyzer. The maximum oxygen concentration could therefore be higher than shown in Figure 9.

The sampling system without oxygen injection was fouled with black tar/char in the tubes, filters, and wash bottles, where the temperature is low enough for tar/char to condense. The sampling system with oxygen injection showed only a few particles in the quartz wool filter, and the liquid in the wash bottles did not contain black particles or other fouling. It was concluded that the probe with oxygen injection was able to reduce the tar/char fouling to an acceptable level that allowed for subsequent reuse of sampling probes and accurate concentration determinations of corrosive constituents.

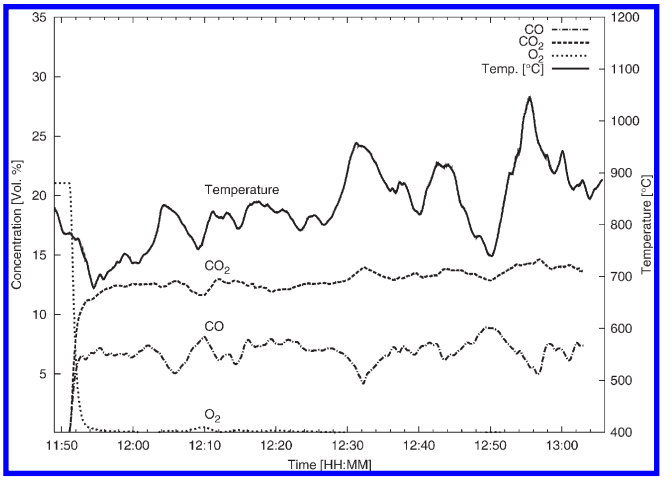

Figure 8. Gas concentration and temperature measurements without oxygen injection at port L2 using probe type S2.

A test run with absorption bottles and oxygen injection using probe type S1 at port L2 was conducted for a period of 2 h and 44 min. The purpose of the test was to validate the capture and the distribution in the absorption system of the elements Cl, S, Ca, K, Na, Pb, and Zn. A volume of 0.1499 m^3 dry flue gas was collected, and 64.21 L of O_2 was injected. Four serially connected wash bottles were used. Two bottles contained a NH_3 solution, and two bottles contained a HNO_3/H_2O_2 solution. The alumina tube was washed with double-distilled water (<18 mΩ conductivity), thus producing

sample number 1. The Teflon tube and the filter were washed, thus producing sample number 2. The next two wash bottles containing NH_3 produced sample numbers 3 and 4, and the last two wash bottles containing HNO_3/H_2O_2 solution generated sample numbers 5 and 6. A baseline test containing double-distilled water was also produced. The samples were analyzed using inductively coupled plasma−optical emission spectrometry (ICP−OES). Table 3 shows the amount of Cl, S, Ca, K, Na, Pb, and Zn in the analyzed samples. It was observed that the supplied baseline test had significantly lower concentrations than the samples from the validation test. It was concluded that the run time was adequate for obtaining samples with concentrations significantly above the background noise.

Table 4 shows the fractional distribution of the sampled constituents in weight percent (wt %). The majority of the constituents are captured in the alumina tube, the Teflon tube and filter, and wash bottles 1 and 2 (WB1 and WB2).

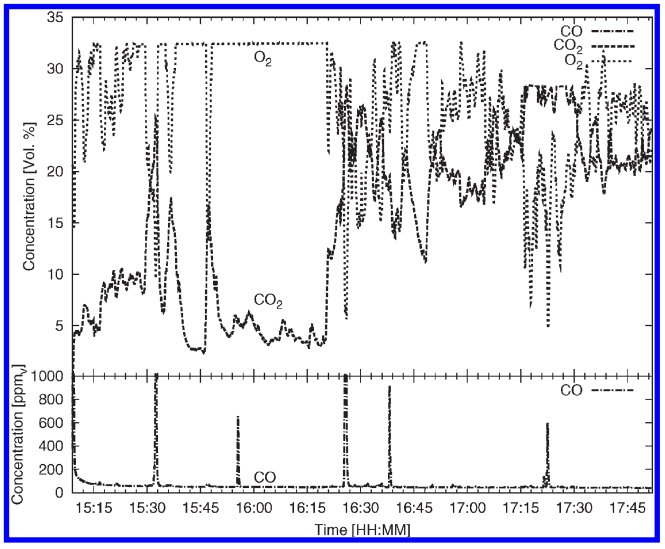

Figure 9. Gas concentration measurement with oxygen injection at port L2 using probe type S1.

For the measured species, less than 5 wt % was found in wash bottles 3 and 4.

For the actual experiments, three wash bottles were used. The first two wash bottles contained the NH_3 solution, and the third wash bottle contained the HNO_3/H_2O_2 solution. The latter wash bottle was not subjected to analysis by ICP−OES. Thus, a less than 5% error was part of the applied analysis method. The reason for accepting this error was the ability to half the number of analyses required because all of the other samples could be combined to one sample. The NH_3 solution could not be mixed with HNO_3/H_2O_2 because that mixture forms NO_2 gas and causes unreliable results in the ICP−OES laboratory equipment.

Flame Position on the Grate. The position of the flame front may influence the local probe measurements. In some of the measurements, it was intended to make a long fire on the grate. However, a long fire appeared somewhat randomly during the measuring campaign; therefore, the video recordings of the grate were used to determine the actual flame front position.

Table 5 shows the average locations of flame positions for each of the probe extractions performed in ports L1−L5 and which type of probe that was used. The standard deviation is a measure for how far the front has been moving back and forth during the experiment. A standard deviation of 1 spans a flame front position spanning the depth of a section. The average flame front position was 3.5, i.e., the middle of section 3 of the grate. The division between a short and long flame was chosen at the middle of section 3, which was the median position number of the video data. For the figures that present the probe measurements, the long flame is marked with filled symbols and the short flame is marked with open symbols.

Temperature Profile. The temperatures above the grate were obtained from the measurements using the S2 and S2* probes. Figure 10 shows the temperature averages and standard deviations for the measurements performed at ports L1−L5 and in the first draft (EBK1). The adjacent numbers are the experimental IDs (see Table 5 for average flame position).

Table 3. Amount of Cl, S, Ca, K, Na, Pb, and Zn in Milligrams Found in Each of the Samples from the Six Different Parts of the Sampling System along with a Baseline Test and the Resulting Concentration in the Dry Flue Gas[a]

	ICP−OES	number 1, Al_2O_3 tube (mg)	number 2, filter and tube (mg)	number 3, WB1 (mg)	number 4, WB2 (mg)	number 5, WB3 (mg)	number 6, WB4 (mg)	baseline test (mg)	flue gas concentration (ppm_v)
Cl	axial	9.6	131.7	68.0	2.0	3.2	1.8	< 0.095	1741
S	axial	14.0	3.3	26.7	0.88	0.68	0.37	< 0.019	409
Ca	radial	5.3	7.9	6.3	0.22	0.088	0.068	0.009	141
K	radial	9.6	11.0	12.4	1.0	1.0	0.65	< 0.038	261
Na	radial	13.1	6.9	7.8	0.87	0.78	0.52	< 0.019	371
Pb	axial	5.3	0.9	0.66	0.087	0.085	0.047	< 0.002	10
Zn	radial	15.8	2.4	2.7	0.22	0.20	0.125	< 0.004	93

[a] This sample originates from port L2.

Table 4. Weight Percentage (wt %) Distribution between Alumina Tube, Teflon Tube and Filter, and Wash Bottles 1−4 for the Validation Test

	Al_2O_3 tube (wt %)	filter and tube (wt %)	WB1 (wt %)	WB2 (wt %)	WB3 (wt %)	WB4 (wt %)
Cl	4.46	60.87	31.44	0.93	1.46	0.83
S	30.44	7.26	58.08	1.93	1.48	0.8
Ca	26.6	39.65	31.85	1.12	0.44	0.34
K	26.95	30.78	34.64	2.88	2.93	1.83
Na	43.77	22.99	25.98	2.9	2.6	1.75
Pb	74.57	13.06	9.27	1.23	1.2	0.67
Zn	73.98	11.03	12.49	1.04	0.92	0.54

Table 5. Overview of Performed Probe Measurements and Video Determination of the Grate Fire Length Sorted by Average ± Standard Deviation[a]

ID	port	probe	average length
		Short Fire Average = 3.1	
8	L4	S1	2.9 ± 0.2
9	L5	S1	2.9 ± 0.2
24	L1	S2	3.1 ± 0.3
25	L2	S2	3.1 ± 0.3
11	L4	S1	3.1 ± 0.4
4	L2	S1	3.1 ± 1.1
5	L4	S1	3.1 ± 1.1
23	L4	S1	3.3 ± 0.2
22	L3	S1	3.3 ± 0.2
6	L4	S2	3.3 ± 0.3
7	L5	S2	3.3 ± 0.3
		Long Fire Average = 3.8	
14	L1	S1	3.5 ± 0.3
15	L2	S1	3.5 ± 0.3
26	L1	S1	3.5 ± 0.6
27	L2	S1	3.5 ± 0.6
19	L3	S1	3.6 ± 0.3
18	L2	S1	3.6 ± 0.3
12	L2	S1	3.6 ± 0.4
13	L3	S1	3.6 ± 0.4
3	L3	S2	3.8 ± 0.3
2	L2	S2	3.8 ± 0.3
20	L3	S2	4.0 ± 0.6
21	L4	S2	4.0 ± 0.6
16	L2	S2	4.3 ± 0.8
17	L3	S2	4.3 ± 0.8
		EBK1 Measurements	
28		S2*	
29		S2*	

[a] Value 1 is the beginning of section 1.0. Value 1.5 is the center of section 1. Value 2.0 is the end of section 1 and the beginning of section 2.

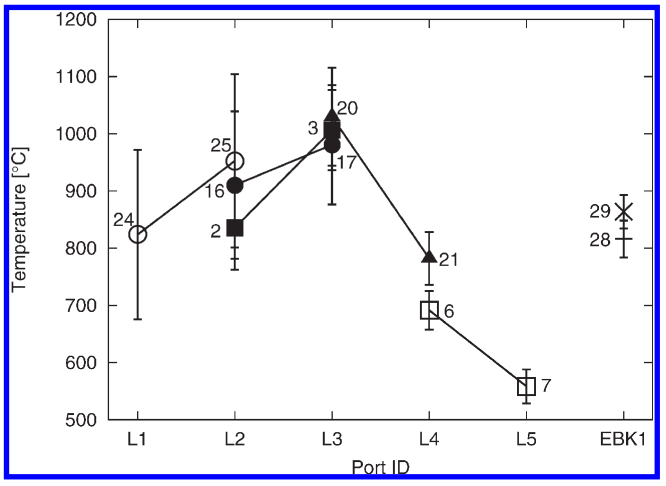

Figure 10. Average temperature measurements and corresponding standard deviations. Filled symbols correspond to long fire (i.e., ≥3.5), and open symbols correspond to short fire (i.e., <3.5).

The temperature generally increased along the grate until it reached port L3, after which it decreased at ports L4 and L5. When the fire was short, the temperature at port 2 was higher than when the fire was long and the temperature at port L4 was cooler. The relatively high temperatures observed at port L4 (692 ± 34 and 782 ± 46 °C) may be caused simultaneously by the cooling of the slags and the ongoing burnout. Measurements have been repeated 3 times at ports L2 and L3 and 2 times at port L4. At L1, greater variations would be expected because of the drying/pyrolysis/combustion taking place at this location, which is also seen by the large standard deviation observed for measurement ID 24.

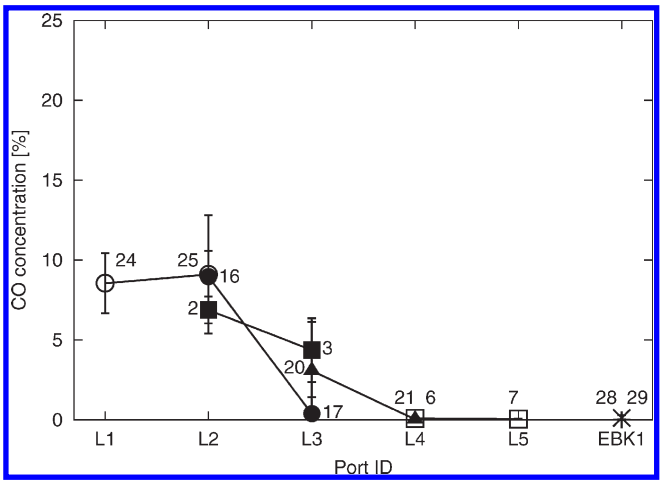

Figure 11. CO measured with no added oxygen to the probe.

The temperature measurements supported the video analysis of the flames ending between ports L3 and L4 during long fire. Even though no visible flames were present and oxygen levels were high (approximately 20%), temperatures remained relatively high at ports L4 and L5 (measurement IDs 6 and 7). The reasons may be that the primary air is heated by the hot slag on the grate. The probe type that was used was a thermocouple in a closed tube, and as such, radiation may be yielding higher temperatures than would otherwise be observed when using a suction pyrometer.

Gas Concentration Profiles. Measurements of gas concentrations were divided into two distinct groups: measurements with injected O_2 and without injected O_2. The measurements at EBK1 (top of first draft) did not use O_2 injection because no tar was present. For all other measurements without injected O_2, only one wash bottle containing ultra-pure water was inserted to reduce tar/char condensation in the rest of the sampling system.

Figures 11−13 comprise results of 14 gas concentration measurements of CO, CO_2, and O_2 with probe S2 with no oxygen injection. Figure 11 shows the CO concentration in the raw grate flue gas decreasing along the grate, with the highest concentrations observed at ports L1 and L2 at ∼9%. At port L3, the level shows large fluctuations because of the flame moving back and forth around the middle of section 3. At ports L4 and L5, concentrations of CO were at parts per million (ppm) levels.

Figure 12 shows the CO_2 concentration in the raw flue gas decreasing along the grate, which can be expected from the CO results. As with the CO concentration, large variations were observed at port L3, after which the concentration decreased to ppm_v levels at ports L4 and L5. Figure 13 shows the concentration of O_2 in the raw flue gas along the grate. O_2 is almost fully depleted at ports L1 and L2, with large variations seen at port L3. The large standard deviations for the O_2 concentrations at port L3 are due to the flame movement. At ports L4 and L5, the oxygen levels are equal to the atmospheric level.

Figures 14 and 15 show the overall average concentrations of $CO/CO_2/O_2$ and NO/SO_2 in the raw flue gas (measurements without O_2 injection), respectively, independent of the flame front position. In Figure 14, the average CO and CO_2 levels

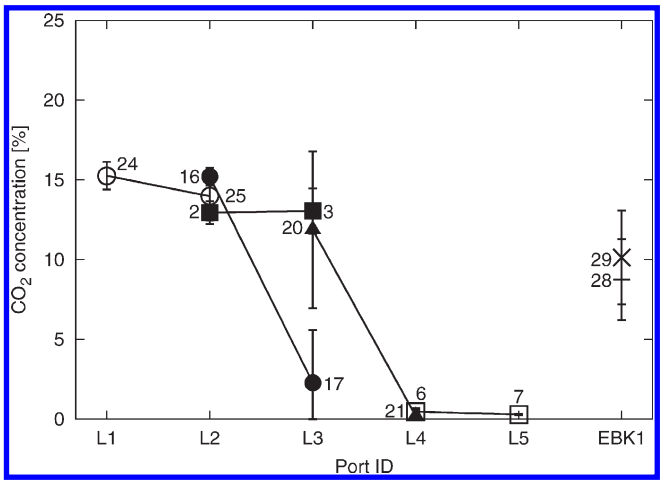

Figure 12. CO_2 measured with no added oxygen to the probe.

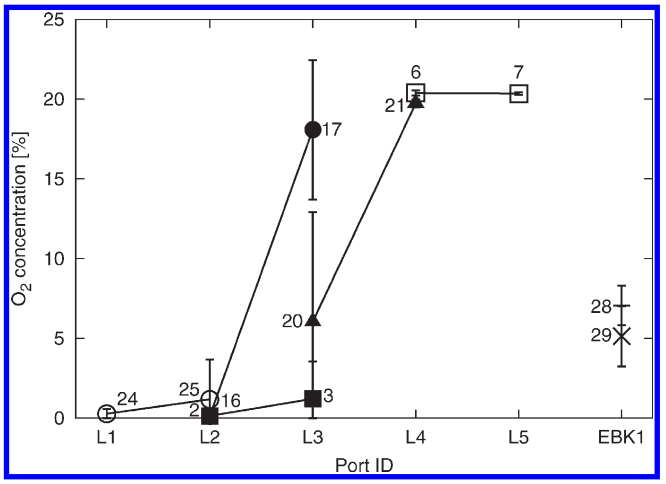

Figure 13. O_2 measured with no added oxygen to the probe.

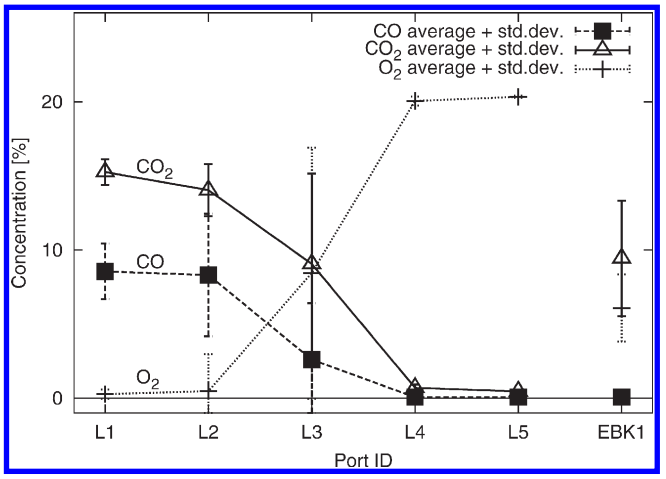

Figure 14. Average values of CO, CO_2, and O_2 along the grate and in the first draft (EBK1) with no O_2 injection.

decrease along the grate, whereas the O_2 level increases along the grate until it reaches atmospheric levels. At ports L4 and L5, little or no combustion was therefore taking place.

The maximum release of SO_2 occurred at port L1, i.e., early on the grate. The largest variations were observed at ports L2 and L3. The SO_2 concentration at port EBK1 in Figure 15 is measured after the flue gas passes an oxidizing

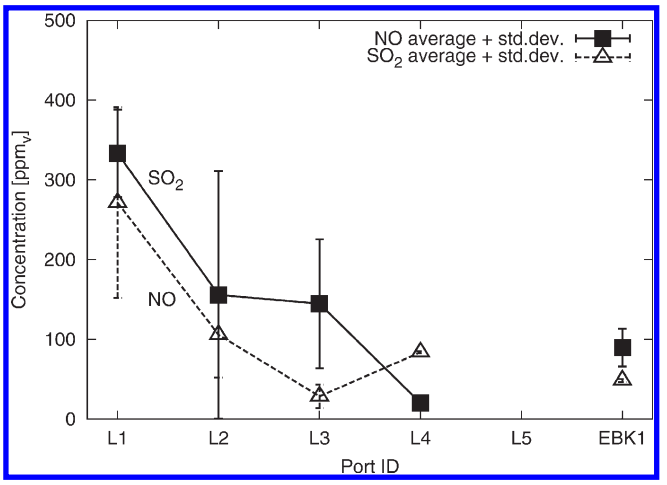

Figure 15. Average values of NO and SO_2 along the grate and in the first draft (EBK1) with no O_2 injection.

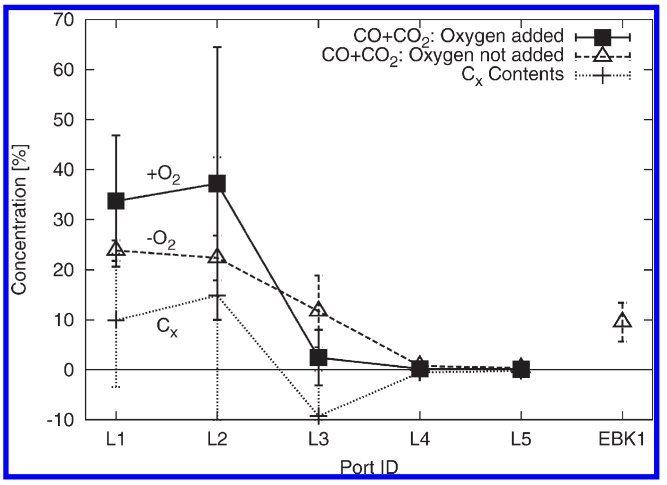

Figure 16. CO and CO_2 and hydrocarbon (C_x) concentrations.

solution, which partially absorbs SO_2. The results from these measurements and the measurements with injected oxygen suggest that most of SO_2 was absorbed by the absorption liquid. In Figure 15, the NO concentration decreases along the grate with relatively large variations on sections L1−L3.

Carbon Release. When CO and CO_2 measurements with and without O_2 injection are compared, it is possible to estimate the release of non-oxidized hydrocarbons from the grate. The CO and CO_2 concentrations with O_2 injection are corrected for the injected O_2. Figure 16 shows the overall averages of the CO and CO_2 concentration measurements with and without oxygen injection for all of the ports. The estimated hydrocarbon concentrations are based on the difference between average measurements of CO and CO_2 with and without injected oxygen. This requires each of the experiments performed at similar combustion conditions to be valid, although this is not possible because of the variations of the flame positions on the fuel bed. It seems that, at ports L1 and L2, there are significant amounts of volatile hydrocarbons in the flue gas. The negative amount determined at port L3 seems to be caused by the flame location fluctuations. It is expected that the hydrocarbon content in the flue gas at port L3 is relatively low compared to ports L1 and L2 because there is a surplus of O_2 present and the CO concentration was low compared to L1 and L2. The share of carbon as hydrocarbons of the total carbon released (CO and

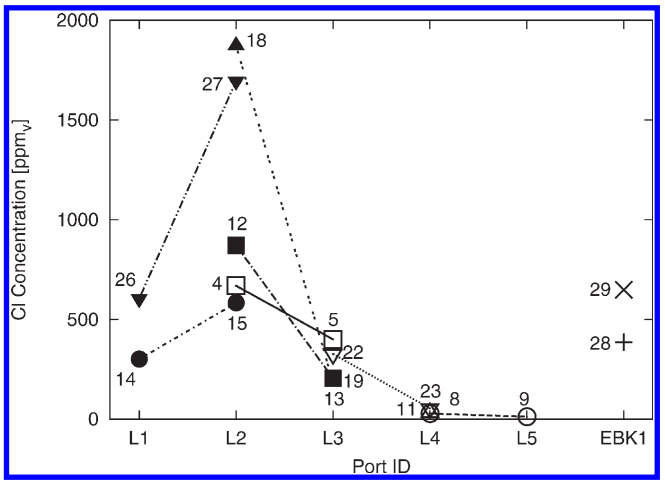

Figure 17. Cl release at ports L1−L5 and EBK1.

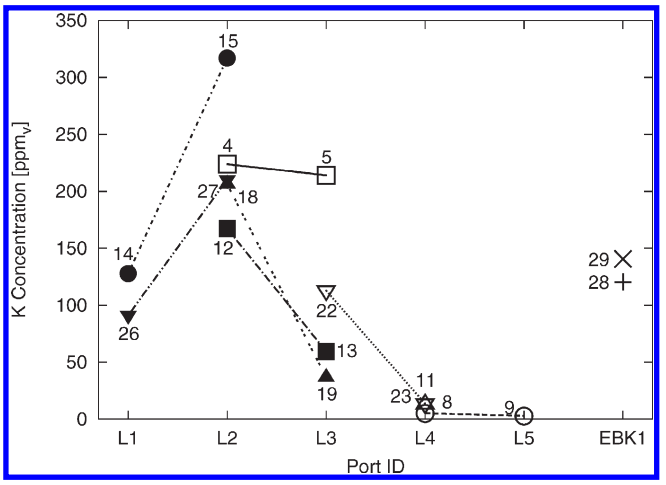

Figure 20. K release at ports L1−L5 and EBK1.

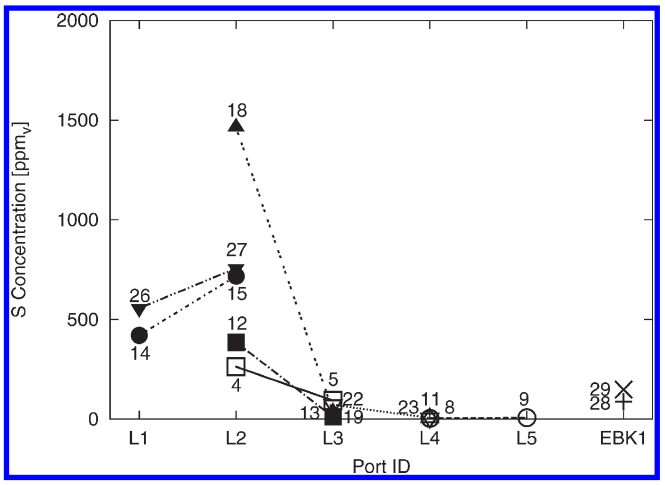

Figure 18. S release at ports L1−L5 and EBK1.

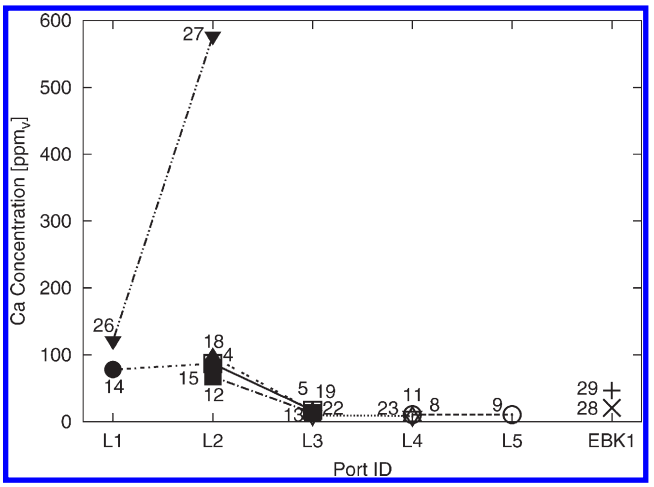

Figure 21. Ca release at ports L1−L5 and EBK1.

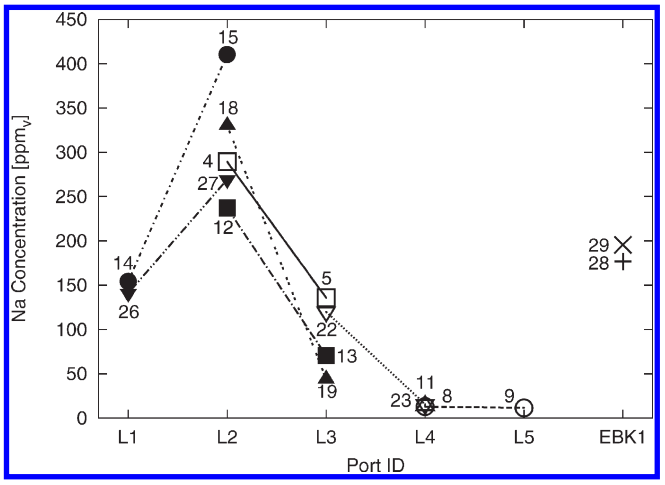

Figure 19. Na release at ports L1−L5 and EBK1.

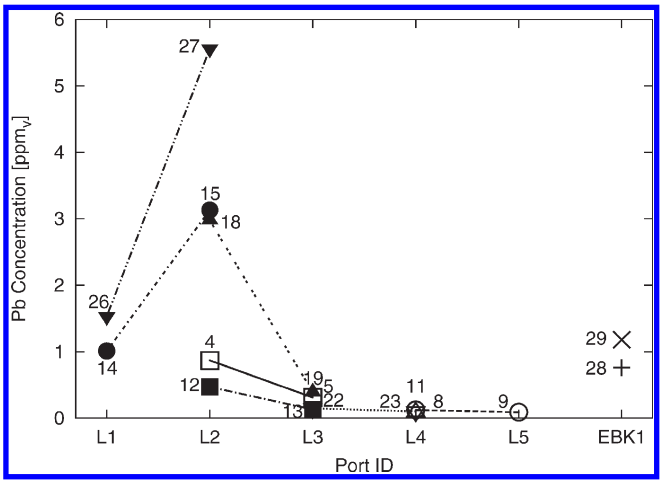

Figure 22. Pb release at ports L1−L5 and EBK1.

CO_2 and C as hydrocarbons) at ports L1 and L2 is 29 and 40%, respectively.

Release Profiles of Corrosive Constituents. In this section, the release profiles along the grate of Cl, S, Na, K, Pb, Zn, Cu, and Sn are shown in Figures 17−25. Figure 17 shows the release of chlorine, and the maximum is observed at port L2. There does not seem to be any clear differences between the short and long grate fire operating conditions. A relatively large difference in the average concentration was observed for the two measurements at the top of the first draft (EBK1). This was not observed for any of the other elements. This may largely be explained by variations in the fuel composition because some polyvinyl chloride (PVC) material may easily cause spikes in the concentration of Cl.

Figure 18 shows the release of S captured by the absorber bottles. The highest release was observed at port L2.

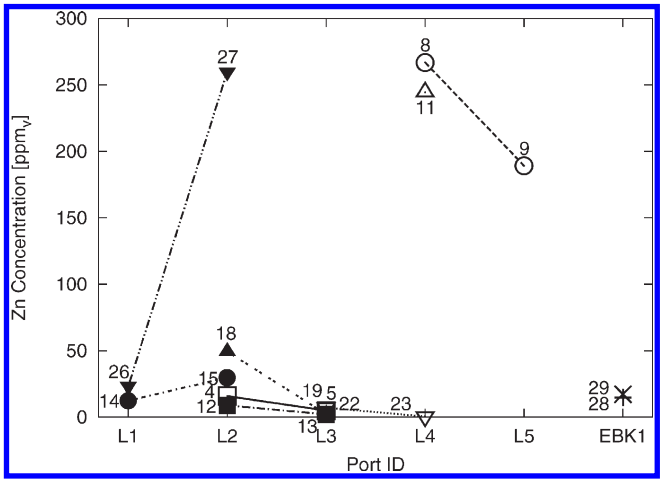

Figure 23. Zn release at ports L1−L5 and EBK1.

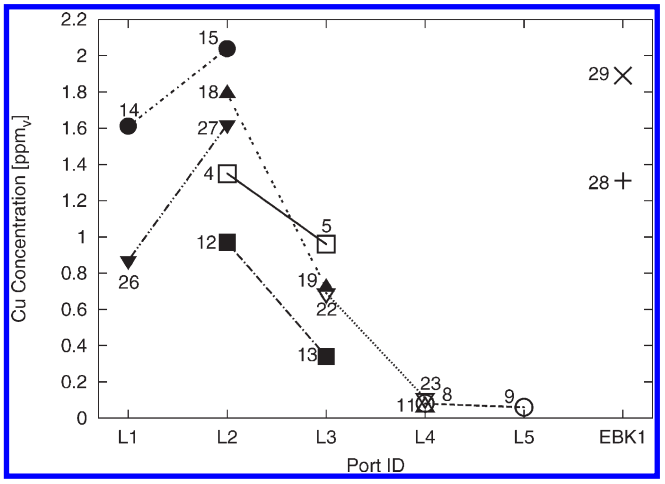

Figure 24. Cu release at ports L1−L5 and EBK1.

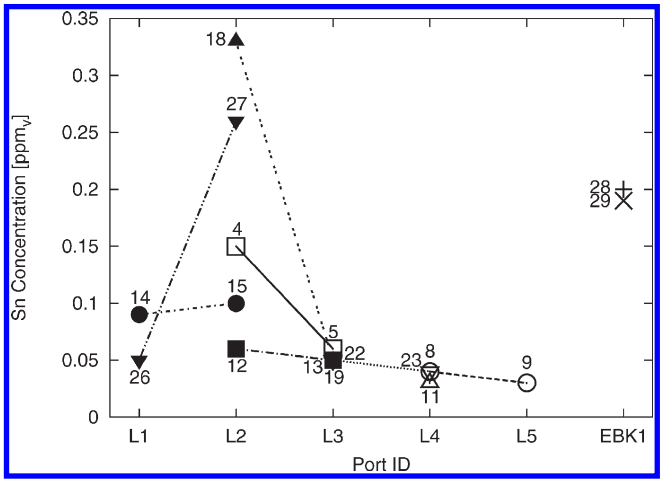

Figure 25. Sn release at ports L1−L5 and EBK1.

There did not seem to be any direct relation between the flame length and release profile. The observed higher level of SO_2 at port L4 from the gas analyzer data (Figure 15) was not reproduced from the wash bottle data. When looking purely at data from the long fire at port L2, large variations in the S concentration are observed. Together with the observed Cl concentration levels, it can be concluded that variations in fuel composition can be the controlling factor of the release of Cl and S during the early stages of combustion on the grate.

Figure 19 show the release of Na along the grate. The maximum release was observed at port L2.

Figure 20 shows the release of K along the grate. The maximum release was observed at port L2.

Figure 21 show the release of Ca along the grate. Except for measurement ID 27 (in which the outer ceramic tube was broken), the concentrations are at or lower than 100 ppm$_v$. This could be interpreted as the oxygen having an effect on the Ca levels in the sample, although that would be very unlikely. Because the outer tube was broken, perhaps not all of the oxygen was entering the tube and the correction by injected volume of O_2 would yield increased values of the concentration for that particular measurement. The effect would be 2-fold: more flue gas would enter, and less O_2 would be extracted with the flue gas.

Figure 22 shows the release of Pb along the grate. The concentration level is low compared to the other major species. A maximum concentration of 5.5 ppm$_v$ Pb is observed at port L2.

Figure 23 shows the release of Zn along the grate. The trend in the graph was in general the same as for many of the other species, except for the relatively high concentration at ports L4 and L5. At port L4, two of three measurements exhibit unusually high levels of Zn. The single measurement at port L5 was also very high. In comparison to the overall concentration measured in the first draft (EBK1), these values did seem to be "incidents" caused by single particles with high concentrations or similar though fuel variations that may also be able to explain the spikes.

Figure 24 shows the release of Cu along the grate. The concentration level was low compared to the other major species. The maximum concentration of 2 ppm$_v$ Cu occurred at port L2.

Figure 25 shows the release of Sn along the grate. The concentration level was low compared to the other major species. The maximum concentration of 0.3 ppm$_v$ Sn occurred at port L2.

Overall Mass Balance. The concentration of different elements in the flue gas were measured in the top of the first draft (EBK1), and it was possible to estimate the flue gas concentration from the measurements performed along the grate. It was also possible to calculate a theoretical flue gas concentration based on the partition of elements from literature data.[10,11]

Table 6 shows the plant data for primary/secondary air flow, waste feed rate, and CO_2/O_2 concentrations in the top of the first draft. The plant data in Table 6 were combined

Table 6. Plant Data for Primary and Secondary Air, Waste Input Feed Rate, and the Wet Concentration of O_2 and CO_2 Measured by Fixed Plant Probes

ID	primary air (N m^3/h)	secondary air (N m^3/h)	waste input (kg/h)	CO_2 (wet %)	O_2 (wet %)
28	101917 ± 4788	11779 ± 922	37729 ± 3763	8.24 ± 0.61	5.19 ± 0.89
29	101262 ± 6093	12006 ± 33	29742 ± 5504	8.25 ± 0.41	5.16 ± 0.62

with literature data[10,11] of the concentration of different elements in waste together with the partitioning of the elements to calculate theoretical flue gas concentrations.

Figure 26 and Table 7 show a comparison of flue gas concentrations of the measured elements Cl, S, Ca, K, Na, Zn, Pb, Cu, and Sn, as well as the non-measured elements Si, Al, and Fe, on the basis of literature data,[10,11] the release from the grate from this investigation, and the measured concentrations at first draft (EBK1).

The Belevi data[10] was based on mixed waste (household and industrial), and the Pedersen data[11] was based on 80% household waste and 20% small combustibles. The most notable difference between the Belevi data[10] and the Pedersen data[11] was the water content of the fuel at 240 and 470 g/kg of fuel, respectively. The Pedersen data were measured during a very rainy season, which was comparable to the very rainy season when these measurements were performed. Furthermore, both plants were Danish, thus contributing to the comparability of the fuels. The Pedersen data however did not contain data for the C, O, and H content in the fuel. The Belevi data were used to supply these data by adjusting them relative to the water contents.

When the literature-based estimated dry concentrations in the flue gas are compared to the measured concentrations in the flue gas at EBK1, it is observed that the data are reasonably similar, except for the Ca measured in EBK1, which was almost an order of a magnitude less than the literature values. However, the literature data are based on fly ash and exit flue gas data, while our measurements mostly quantify gas-phase species. The differences between the estimated concentration values based on the grate measurements and the measured values at EBK1 were both negative and positive depending upon the elements.

The flue gas concentration data based on the grate measurements are generally lower, although not significantly lower, than the concentrations measured at EBK1. Generally, the EBK1- and grate-based data agree within a factor of 2; however, larger deviations are observed for the elements Na, Zn, and Sn. We believe that the differences probably mainly originate from variations in the fuel composition, although the sampling technique may also be an additional cause to variations between measurements where gas/solid conditions are not similar.

In a previous study,[8] the concentrations of Cl, Na, Ca, K, CO_2, CO, and O_2 above the grate in the same boiler were also measured. The levels of CO, CO_2, and O_2 were on a similar level, while the concentrations of Cl, K, and Na were found to be at a lower level in port L2 in the old study. We believe that the difference in the measured port L2 levels can be

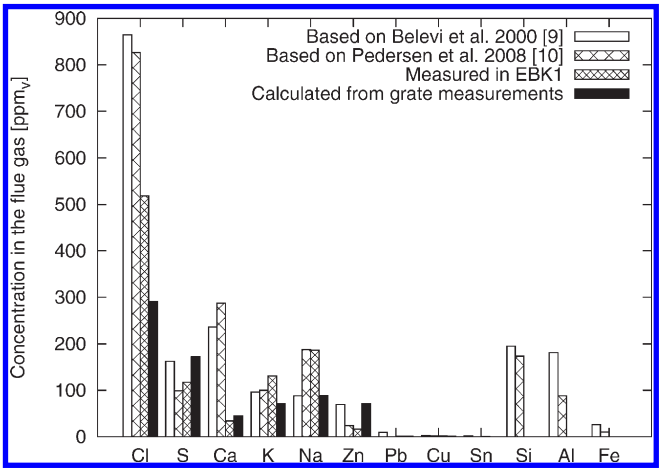

Figure 26. Theoretical flue gas concentrations compared to the measured concentration.

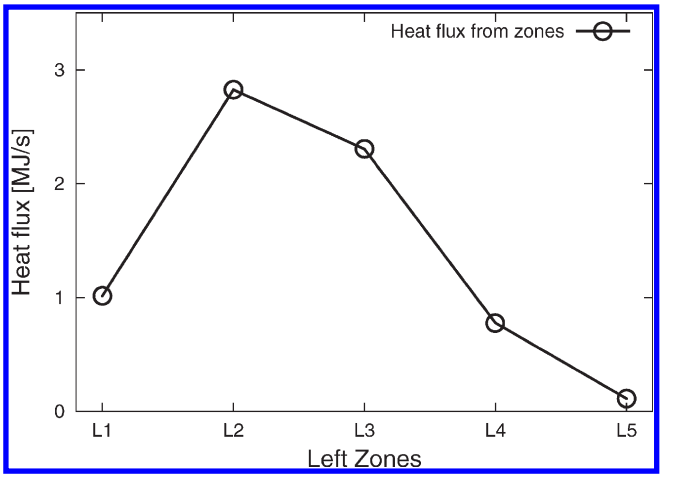

Figure 27. Potential average heat release from the grate sections calculated using a base temperature of 500 °C.

Table 7. Concentrations in the Flue Gas Based on Stoichiometric Concentrations Calculated from Literature Data, Measured Concentration, and Estimated from the Grate Release Concentrations[a]

element	on the basis of ref 10 concentration, dry (ppm$_v$)	on the basis of ref 11 concentration, dry (ppm$_v$)	EBK1 concentration, dry (ppm$_v$)	grate-based concentration, dry (ppm$_v$)	L2 concentration, dry (ppm$_v$)	L3 concentration, dry (ppm$_v$)	L4 concentration, dry (ppm$_v$)
Cl	865	827	518 ± 185	291	1138 ± 602	279 ± 102	37 ± 14
S	162	99	117 ± 43	171	717 ± 468	53 ± 36	4.7 ± 0.9
Ca	236	287	34 ± 18	45	183 ± 221	14 ± 3	8.7 ± 1.7
K	96	100	131 ± 14	71	225 ± 56	106 ± 79	11 ± 5
Na	88	187	186 ± 13	88	307 ± 67	93 ± 43	14 ± 1
Zn	69	24	16 ± 2	70	73 ± 106	4.1 ± 2.4	171 ± 148
Pb	9.3	0.14	0.97 ± 0.3	0.62	2.6 ± 2.0	0.25 ± 0.13	0.10 ± 0.02
Cu	2.4	1.1	1.6 ± 0.4	0.53	1.6 ± 0.4	0.68 ± 0.26	0.08 ± 0.03
Sn	1.9	0.12	0.2 ± 0.01	0.06	0.18 ± 0.11	0.05 ± 0.01	0.04 ± 0.01
Si	195	173					
Al	181	88					
Fe	26	10					
volumetric percentages (vol %)							
O_2	1.5	6.4	6.1 ± 2.3				
CO_2	15.8	8.9	9.4 ± 3.9				

[a] Local concentrations at L2−L4 are also shown to compare to the global concentrations.

attributed to the use of a probe in the old study,[8] where some alkali species were embarked in tar species.

Heat Release Profile. Figure 27 shows the average theoretical heat release from the grate zones. The available heat flux from the grate zones was calculated on the basis of the temperature measurements and information on the grate section air flows.[8] The calculated heat flux from the grate zones is the same from the heat of reaction of CO and O_2 and the energy for cooling of the flue gas to 500 °C. The potential contribution from the oxidation of hydrocarbons is not included. The overall maximum energy release was observed at port L2.

The concentration of corrosive constituents in the flue gas from grate section 3 is much lower than the measured concentration at EBK1. The heat flux from section 3 is relatively high and could provide the driving force to elevate the superheater steam temperature. The concentrations at port L3 were in general about half of those measured in EBK1. Combining the flue gases from sections 3 and 4 could provide dilution of the flue gas before passing an inserted superheater section.

Conclusion

Measurements of local gas concentrations (CO, CO_2, O_2, NO, and SO_2), volatile constituents (Cl, S, Na, K, Ca, Pb, Zn, Cu, and Sn), and gas temperature were conducted along the grate of a grate-fired waste incineration plant. The plant had six ports along the grate, of which measurements were performed in the first five ports. Measurements were also performed in a port in the top of the first draft in the fully mixed flue gas. Video recordings of the grate fire were used to document the location of the visible flames during the experiments.

A new probe was designed to conduct measurements in a flue gas with a high tar content. Oxygen injection in the tip of the probe was used to combust the tar. The newly designed probe with added oxygen was reliably producing extraction samples that could be analyzed directly by ICP−OES. The samples that originated from the same port yielded reasonably similar concentrations.

The position of the flame front on the grate may influence the local probe measurements. In some of the measurements, it was intended to make a long grate fire. However, a long fire appeared somewhat randomly during the measuring campaign; therefore, the video recordings of the grate were used to determine the flame front position. The division between a short and long flame was chosen at the middle of grate section 3, which was the median flame position number of the video data. The impact on the temperature is observed at port L2, where shorter length of flames yield higher temperatures. Longer flames yield higher temperatures at port L4. No short flame temperature measurements were performed at port L3, although lower temperatures would have been expected. The length of the flames did not seem to make a significant difference between the concentration measurements of corrosive species. The authors believe that this is due to the design of the grate that does not allow for much mixing of the waste along the grate.

The local temperature was measured using a closed tube containing a thermocouple. The temperatures at ports L1 and L2 were 824 ± 148 and 900 ± 212 °C, respectively, and the maximum temperature was measured at port L3 to be 1006 ± 152 °C. At the port in the first draft (EBK1), a temperature of 840 ± 43 °C was measured.

Gas concentration measurements showed nearly no oxygen in the flue gas at ports L1 and L2 (0.3 and 0.5 vol %), some at port L3 (8.5 vol %), and approximately 21 vol % at ports L4 and L5. Likewise, the CO concentration at ports L1, L2, and L3 were 8.6, 8.3, and 2.5 vol %, respectively, and below 0.3 vol % at ports L4 and L5. The primary air rises vertically through the fuel bed, where different stages of combustion occur. Early on the grate, much CO is present because of sub-stoichiometric conditions with drying and pyrolysis as the prevailing processes. These processes have shifted slightly at port L2 with higher temperatures but with sub-stoichiometric conditions. At port L3, char combustion is the prevailing process with little pyrolysis, which was also indicated by the highest temperatures measured at port L3 and a surplus of oxygen. At ports L4 and L5, O_2 is higher than 20 vol %, i.e., indicating that the gas above the grate is heated mainly by cooling the hot slag on the grate and that combustion is limited at grate sections 4 and 5.

When the gas concentration measurements with and without oxygen addition are combined, it was possible to estimate the local carbon concentrations, C, in the form of tar at ports L1−L3. At port L1, the carbon concentration was estimated to be approximately 10 mol %, and at port L2, this number was approximately 15 mol %. At port L3, nothing could be directly concluded because of large variations in the position of the grate fire. It can be concluded that large amounts of hydrocarbons are released from the first two grate sections.

An important objective of this study was to quantify the release of the elements Cl, S, Na, and K along the grate. These elements appear in corrosive ash deposits, and a flue gas with a lower concentration of Cl, S, Na, and K is less corrosive.[12,13] For all of the elements, the maximum concentrations were measured at port L2, followed by a steep decrease at ports L3 and L4. The measured maximum concentrations of Cl, S, Na, and K were approximately 1800, 800, 350, and 250 ppm_v, respectively.

The patent idea (Figure 1) that initiated this study was to use a part of the flue gas from the grate that has low concentrations of corrosive constituents and a sufficient enthalpy to make a high-temperature steam superheating possible. The conducted measurements show that flue gas from grate sections 3 and 4 can produce a sufficiently hot flue gas that only contains low concentrations of corrosive species. It will, however, require a steady control of the position of the grate fire to the flue gas for extra steam superheating.

Acknowledgment. The project was funded by Energinet.dk under contract PSO 6368. The authors thank the technical staff at Vestforbrænding for their help during the experiments.

(10) Belevi, H.; Moench, H. *Environ. Sci. Technol.* **2000**, *34*, 2501–2506.
(11) Pedersen, A. J.; Frandsen, F. J.; Riber, C.; Astrup, T.; Thomsen, S. N.; Lundtorp, K.; Mortensen, L. F. *Energy Fuels* **2009**, *23*, 3475–3489.
(12) Grabke, H. J.; Reese, E.; Spiegel, M. *Corros. Sci.* **1995**, *37*, 1023–1043.
(13) Spiegel, W.; Herzog, T.; Magel, G.; Muller, M. W.; Schmidl, G. W. *VGB PowerTech* **2005**, *85*, 89–97.